Polarization of poly(vinylidene fluoride) and poly(vinylidene fluoride-trifluoroethylene) thin films revealed by emission spectroscopy with computational simulation during phase transition

Vladimir S. Bystrov, Ekaterina V. Paramonova, Yuri Dekhtyar, Robert C. Pullar, Aleksey Katashev et al.

Related Articles

Additional information on J. Appl. Phys.

Polarization of poly(vinylidene fluoride) and poly(vinylidene fluoride-trifluoroethylene) thin films revealed by emission spectroscopy with computational simulation during phase transition

Vladimir S. Bystrov,[1,2,a)] Ekaterina V. Paramonova,[2] Yuri Dekhtyar,[3] Robert C. Pullar,[1] Aleksey Katashev,[3] Natalie Polyaka,[3] Anna V. Bystrova,[4] Alla V. Sapronova,[5] Vladimir M. Fridkin,[6] Herbert Kliem,[7] and Andrei L. Kholkin[1]

[1]*Department of Ceramics & Glass Engineering & CICECO, University of Aveiro, 3810-193 Averio, Portugal*
[2]*Institute of Mathematical Problems of Biology RAS, 142290 Pushchino, Russia*
[3]*Institute of Biomedical Engineering and Nanotechnology, Riga Technical University, LV-1658 Riga, Latvia*
[4]*Institute of Theoretical and Experimental Biophysics RAS, 142290 Pushchino, Russia*
[5]*Bergen Center for Computational Science, Unifob AS, N-5008 Bergen, Norway*
[6]*Institute of Crystallography, RAS, 59, Leninsky Pr., 933333 Moscow, Russia*
[7]*Institute of Electrical Engineering Physics, Saarland University, D-66041 Saarbrücken, Germany*

The electronic structure and self-polarization of P(VDF-TrFE) Langmuir-Blodgett nanofilms were analyzed under temperature-driven phase transitions, according to their thickness, composition, and structural conformation. Both thermo-stimulated exoelectron emission (TSEE) spectroscopy and computational simulation, including quantum-chemical calculations from first principles, were carried out. PVDF and composite P(VDF-TrFE) (70:30) molecular chains as Trans and Gauche conformers, as well as crystal cells, were modeled for these TSEE analyses. The quantum-chemical calculations and the computational simulation were based on the density functional theory (DFT) as well as semi-empirical (PM3) methods. It was demonstrated that the energy of electron states, as well as the total energies of the studied P(VDF-TrFE) molecular clusters during phase transformation, is influenced by electron work function and electron affinity. Analysis was performed by combining TSEE experimental data with the computational data of the molecular models, demonstrating the effectiveness of this joint approach. For the first time, TSEE was used for contactless measurements of nanofilm polarization, and characterization of the phase transition. The proposed new method can be widely applied in nanobiomedicine, particularly in development of new bone bio-implants, including built-in sensors (new smart nanotechnology). © *2012 American Institute of Physics*. [http://dx.doi.org/10.1063/1.4721373]

I. INTRODUCTION

Ferroelectric Langmuir-Blodgett (LB) thin films, based on the poly(vinylidene fluoride) (PVDF) and poly(vinylidene fluoride-trifluoroethylene) (P(VDF-TrFE)) copolymers, have demonstrated polarization switching phenomena on the nanoscale, with local ferroelectric polarization reversal on the atomic-molecular level.[1–5] These LB polymer films are now being widely explored, using various techniques, including nanoscale characterization by piezoresponse force microscopy (PFM).[6–11] They are of interest as novel prospective ferroelectric nano-materials for applications in nanotechnology and microelectronics, data storage, and new non-volatile memory cells.[12] In biomedicine and nanomedicine, they are promising components of various nanocomposites due to their acoustic and piezoelectric properties, and have a high compatibility with many organic and biological molecules and tissues.[13–18] Nevertheless, many of the important physical and structural properties of PVDF copolymer thin films are not yet clearly understood. This is especially true for polarization switching phenomena in various conditions and compositions. One promising idea is to use actuators made from biocompatible PVDF piezoelectric materials. Such an actuator could be placed onto a bio-implant's surface, to encourage bone growth by electrical and mechanical stimulation of osteoblast cells,[19,20] due to the high surface charge—polarization of PVDF and P(VDF-TrFE). As such, they are similar to recently developed highly polarized (surface charged) hydroxyapatite (HAP).[21,22] It has been showed that the number of attached osteoblasts sharply increases on the negatively charged HAP surface.[23]

It is well known that in ferroelectrics, polarization is coupled with piezoelectric constants.[24] The use of PVDF means that the mechanical stimulation of bone growth depends on the amount of electrical energy applied, and that bone growth can be stimulated in different directions by changing piezoelectric constants. This concept of smart structures can be adapted to other active devices. In this case, it is necessary to know the mechanisms of charging (polarization formation) and to be able to control them. It is important not to distort the dynamics of the behaviour of the controlled object during analysis.

Such non-contact measurements of the surface charge (polarization) can be performed by the method of thermo-stimulated exoelectronic emission (TSEE),[25–27] which allows us to measure changes in work function, and determine the

a)Author to whom correspondence should be addressed. Electronic addresses: bystrov@ua.pt and vsbys@mail.ru.

value of surface charge (polarization). For correct determination of the polarization, it is necessary to have a corresponding correct molecular model for the mechanisms of the processes occurring in the surface layers of the sample. For this reason, computational modeling from first principles and studies for several structures of the PVDF and P (VDF-TrFE) molecular models at different phase conformations—trans (T) and gauche (G)—have been performed. The appropriate structures of the two states of the sample—in a polar ferroelectric phase and a nonpolar paraelectric phase—were determined, corresponding to the molecular models of P(VDF-TrFE) crystal cells in the trans and gauche conformations. The data thus obtained allow us to calculate electronic spectra and construct diagrams of energy bands for these two different phases, as well as determine the band gap (forbidden energy band) and its changes during phase transition. It is important to note that the variations in these parameters depend on the internal electric field which appears on the surface, as a function of surface charge (polarization). On the other hand, the changes of the surface charge alter the work function measured by TSEE, and in different phases (and conformations) these changes have different effects. The model thus created, based on the energy band structures and their changes during phase transition, allows non-contact measurement of polarization through the work function data, measured by TSEE.

In this paper, we report on our studies of the polarization properties of P(VDF-TrFE) copolymer films by the use, for the first time for these purposes, of a novel contactless method—TSEE analysis,[25–27] coupled with molecular modeling from first principles. These studies continue the series of our previous investigations of ferroelectric and nanoscale properties of thin LB PVDF copolymer films.[11,16–18] The proposed new method can be widely used in bionanomedicine, particularly in the development of new bone bio-implants, incorporating built-in sensors (new smart nanotechnology).

II. EXPERIMENTAL DETAILS

The preparation, structure, phase transitions, and ferroelectric properties of P(VDF-TrFE) films prepared by LB method were described in detail in Refs. 1–3. They manifest spontaneous polarization $P_s \sim 0.1$ C m^{-2} in the polar "2 mm" orthorhombic phase (according to standard crystallographic classification). At 80–100 °C (depending on the proportion of VDF to TrFE), the copolymer passes into the nonpolar "6 m" hexagonal phase via a first-order phase transition. High-quality thin films of ferroelectric P(VDF-TrFE) (70:30) were produced by the LB method using the horizontal Schafer variation of the LB technique. The optimal surface pressure on the isotherm chosen was 6 mN m^{-1}. P(VDF-TrFE) powder from Piezotech Inc. of concentration 0.1 g/l was used. The samples were prepared in Saarbruecken and had structures formed from 10, 20, 30, and 50 depositions onto the glass substrate.[4,5] For this work, we used the samples with 10 and 30 depositions from this series. Film thickness was determined by both ellipsometry[4,5] and atomic force microscopy (AFM) techniques.[6,11] For the prepared samples,

it was determined that one transfer corresponded to one monolayer (ML) with an average thickness of 0.5 nm.[4,5]

For structural characterization of the films in this work, atomic-resolution scanning tunnelling microscopy (STM) was used, the images showing that the films had excellent crystalline structure with the polymer chains parallel to each other in the plane of the film. The structure of LB films has previously been studied by means of x-ray and neutron diffractometry, as well as STM.[1–3] Additionally, AFM, and especially PFM, was used for detailed structural characterization of the films' surface and width. Such PFM measurements were performed, and both topography and piezoelectric images taken at the University of Aveiro using a commercial scanning force microscope (Multimode, Nanoscope IIIA, Veeco) equipped with a function generator and lock-in amplifier.[6,11] No piezoelectric contrast or domains could be found on the piezoelectric image before application of a voltage (writing), just a weak background signal that could be due to either self-polarization of the surface layer or an apparent signal generated by the contact potential difference between the tip and bottom electrode.[11]

Thermo-stimulated exoelectron emission was recorded with a photoelectron emission spectrometer for measurements in a vacuum chamber with a pressure of 10^{-4} Pa. The heating rate of the samples was 0.4 °C/s. When necessary, additional photo-stimulation of samples was provided by ultraviolet (UV) illumination from a deuterium source (DDS-30 D lamp). The required photon energy was selected by means of a SF-26 monochromator. The frequency width did not exceed 0.08 eV. The values of measured work function Φ were estimated with an uncertainty that did not exceed ± 0.04 eV. For measurement of the electron emission, a very sensitive electron detector was used. The secondary electron multiplier had a noise current of 0.1-1 electron/s.[27]

III. TSEE: RESULTS, ANALYSIS, AND DISCUSSION

Thermo-stimulated exoelectron emission analysis has been employed for the measurement of polarization of P(VDF-TrFE) specimens in a novel non-contacting mode. TSEE is very suitable method for the characterization of the surface electronic structure of P(VDF-TrFE) films with different thickness and compositions. TSEE from dielectric and non-metallic materials is typically provided by the thermo-electron emission mechanism,[25–27] with the temperature (T) dependent processes in the emitter being the modulation factor of the electron emission current (I). In the case of ferroelectric PVDF or P(VDF-TrFE) films, the polarization/depolarization follow this modulation factor. Therefore, the features of the I(T) behavior also characterize depolarization of the P(VDF-TrFE) film. In the case of our ferroelectric thin films, deposited on the dielectric glass substrate (without any metallic electrodes), the electron energy zone distributions, their tilt and shift, are schematically presented in Fig. 1.

The TSEE spectra of P(VDF-TrFE) films, having thicknesses of 10 (10 ML) and 30 (30 ML) monolayers (or with ~5 nm and ~15 nm thickness, respectively) deposited onto a glass substrate, were measured. The TSEE spectra are shown in Fig. 2(a). The 30 ML film demonstrates a maximum (at
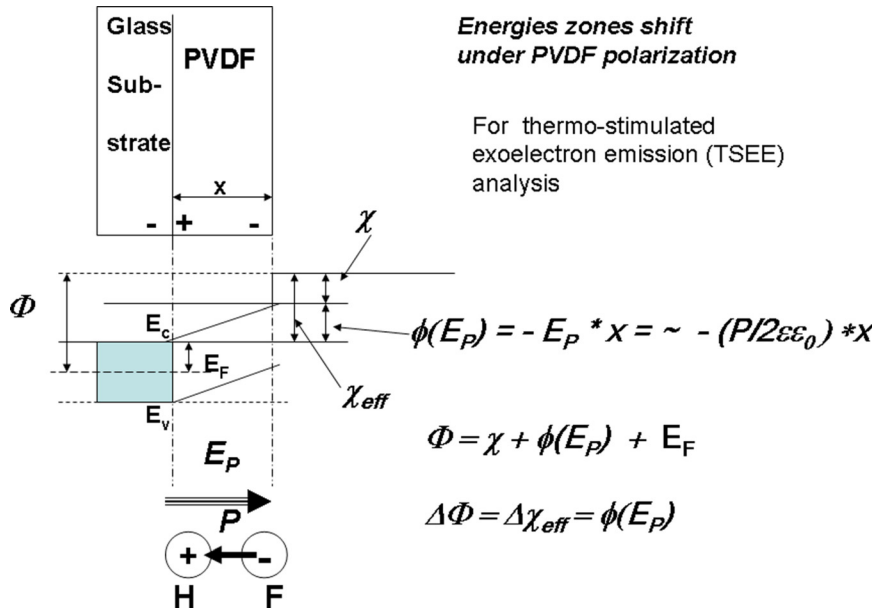
FIG. 1. Schematic of energy zones, and their shift under the influence of an electric field, from polarization of PVDF or P(VDF-TrFE) thin films deposited on a glass substrate: Φ, thermo-electronic emission work function; χ and χ_{eff}, affinity and the effective affinity of an electron; ϕ, energy of electric field E_P inside of PVDF or P(VDF-TrFE) film with polarization P and thickness x; E_F, energy of Fermi level; E_c and E_v, energies of the conductance and the valence bands in the PVDF or P(VDF-TrFE) film.

$T_{max} = +100\,°C$), in contrast to the 10 ML film. This means that the 10 ML film does not undergo any reorganization and polarization under heating, while the 30 ML film does. Because both P(VDF-TrFE) and the glass substrate are insulators, the electrons could escape from both P(VDF-TrFE) and the glass local states, and so there is not enough T to provide thermo induced emission from the valance band for the 10 ML film. Taking into account the thermo electron emission mechanism of TSEE, the maximum in 30 ML could

have resulted from competition between the increased probability of thermo emission and the decreased density of the electrons in the local states; both of these processes are being driven by T. When $T < T_{max}$, the emission of electrons is influenced by the electrical field of polarization (self-polarization). However, at $T > T_{max}$, the thermally induced depolarization "switches off" the electrical field. In this case, the thermo emission electron work function Φ should become smaller. To verify this, the value of Φ was estimated using the following equation for the thermo emission current:

$$\ln\frac{I}{T^2} = \ln A - \frac{\Phi}{kT}, \qquad (1)$$

where A is the emission coefficient, and k is the Boltzman constant. The plots of (1) for the 30 ML film are presented in Fig. 2(b). The values of Φ calculated from Fig. 2(b) were equal to 1.97 eV at $T < T_{max}$, and 0.72 eV when $T > T_{max}$. This result (the decrease of Φ when $T > T_{max}$) supports the model proposed above. Moreover, the temperature induced depolarization corresponds with the change of the potential, $U_P = 1.97 - 0.72 = 1.25$ eV. The corresponding internal electrical field, E_P, with a distance x equal to 15 nm (30 ML) can be calculated: $E_P = 1.25$ eV/15 nm $= 0.083$ eV/nm $= 8.3 \times 10^5$ eV/cm $= 0.83$ MeV/cm. This electrical field resulted from the 30 ML P(VDF-TrFE) film's internal self polarization.

This polarization in P(VDF-TrFE) films shifts the electron energy zones and the thermo-electron work function, Φ, as well electron affinity, χ, for the case of a plane model of thin P(VDF-TrFE) film with thickness x, as represented in Fig. 1. The resultant change of the electron potential energy, $\phi(E_P)$, could be written as the following:

$$\phi(E_P) = -E_P \cdot x = -\frac{P}{2\varepsilon\varepsilon_0} \cdot x, \qquad (2)$$

where ε is the dielectric relative permittivity, and $\varepsilon_0 = 8.8541878 \times 10^{-12}$ C/Vm (permittivity of free space). Therefore, the spontaneous polarization, P, inside this P(VDF-TrFE)
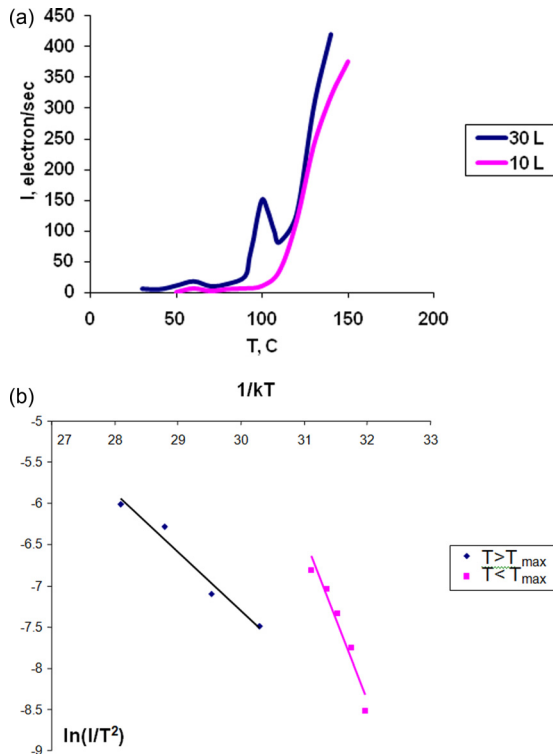

FIG. 2. TSEE spectra of the P(VDF-TrFE) films deposited on the glass substrate: (a) the P(VDF-TrFE) films with a thickness of 10 (10 ML) and 30 (30 ML) monolayers; (b) the fitted lines of Eq. (1) for the 30 ML film.

film could be expressed in absolute values as $P = 2\varepsilon\varepsilon_0 E_P$. For 30 ML P(VDF-TrFE) films having a thickness of $x = 15$ nm, the polarization value, estimated for $\varepsilon \sim 10$ (see, for example, ε data from Refs. [1], [2], and [28]–[32] for P(VDF-TrFE)), is $P = 0.0147$ C/m^2 ~ 1.5 μC/cm^2. From[4,5] data (for a similar 30 ML P(VDF-TrFE) (70:30) sample with a thickness of d $= 16.3$ nm (at T $= 273$ K)), polarization was ~ 5–7 μC/cm^2. However, these data were directly after polarization in an applied electrical field, while in our case we have data without an applied electrical field (self-polarized), and after a long relaxation time. It is known that in similar PVDF films, with a relaxation time of ~ 1 h the polarization value decays by 40%–50%,[3,4] so these reported values could be expected to lower to ~ 2–3 μC/cm^2 after 1 h, and after long storage periods P may decrease to ~ 1 μC/cm^2, which is close to the value in our case.

An attempt was also made to polarize the 10 ML film, by radiating the specimen with UV light. Simultaneously, an uncoated glass substrate was radiated and tested by photo-electron emission analysis, to estimate an increment of the induced electrical field, the photoemission work function, Φ_{pe}, being the index of this. Φ_{pe} was derived using the photo-emission current, I_{pe}, equation:

$$I_{pe} = (E_p - \Phi_{pe})^m, \qquad (3)$$

where E_p is the energy of the photon, and m is a power index.

UV radiation increased the value of Φ_{pe} from 5.1 eV to 5.2 eV, meaning that the surface of the glass substrate had been charged negatively (see Fig. 1). After this UV radiation, the TSEE of this P(VDF-TrFE) sample demonstrated a maximum at $T_{max} = +120\,^\circ$C (Fig. 3(a)). The lines (1) for the 10 ML film are shown in Fig. 3(b). The values of Φ calculated from Fig. 3(b) were equal to 1.34 eV at $T < T_{max}$ and 0.08 eV for $T > T_{max}$. Again, the result (decrease Φ when $T > T_{max}$) is in favor of the TSEE model above. Because UV radiation provided the potential by $5.2 - 5.1 = 0.1$ eV, the true potential from the P(VDF-TrFE) film is equal to $1.34 - 0.1 = 1.24$ eV. Therefore, the temperature depolarized the film from 1.24 eV to 0.08 eV, i.e., $U_P = 1.16$ eV, corresponding to the electrical field of polarization, E_P, for a distance of $x = 5$ nm (10 ML), giving $E_P = 1.16$ eV/5 nm $= 0.232$ eV/nm $= 23.2 \times 10^5$ eV/cm $= 2.32$ MeV/cm. As result, the P(VDF-TrFE) sample with 10 ML, which had no initial P, demonstrated a polarization with $E_P \sim 23.2 \times 10^5$ V/cm from TSEE measurements, after UV radiation.

Comparing this number with the 8.3×10^5 V/cm obtained for the 30 ML P(VDF-TrFE) film, one can conclude that

1. The 30 ML P(VDF-TrFE) film, in contrast to the 10 ML one, is self polarized.
2. The 10 ML P(VDF-TrFE) film has a capacity for polarization induced by UV radiation with an induced polarization 2.8 times higher than that of the 30 ML self polarized film.

The corresponding value of polarization for the 10 ML film (for $\varepsilon = 10$) is $P = 0.0418$ C/m$^2 = 4.2$ μC/cm^2. This
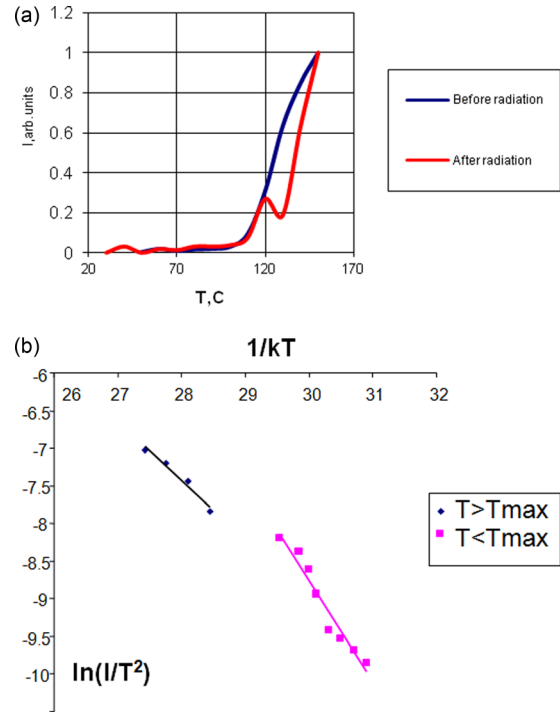

FIG. 3. TSEE spectra of the 10 ML P(VDF-TrFE) films deposited on the glass substrate: (a) the 10 ML P(VDF-TrFE) films before and after radiation; (b) the fitted lines of Eq. (1) for the 10 ML film.

value agrees with the previously reported measured polarization data for similar samples of ~ 4–6 μC/cm^2.[4,5]

This also explains why these values of induced P for 10 ML films are larger than our data for a 30 ML self polarized sample, while usually the sample with more MLs would be expected to have the greater polarization. The radiation excites electrons to a conductance band in the glass substrate (charging the glass surface with negative potential), and also from the P(VDF-TrFE) valence band, because for PVDF and P(VDF-TrFE) the energy gap, E_g, ~ 5.1–5.6 eV,[31–37] close to the energy of the photons used ($E_{pe} \sim 5.2$–5.3 eV). However, data on various glass types show an energy in the order of $E_{pe} \sim 6$–12 eV,[38] and only in the case of glass with a Fe$_2$O$_3$ admixture does $E_{pe} \sim 5.3$–5.4 eV. This suggests that the excited electrons which occupied conductance bands were mainly from the region of the thin P(VDF-TrFE) film. Another possibility connected to the existence of trapped levels close to the bottom of the conductive band (i.e., P(VDF-TrFE) as a *n*-type semiconductor) is discussed in Sec. IV.

However, it must be emphasized that our direct experiments with an uncoated glass substrate showed that its surface was negatively charged after UV illumination. Therefore, excited charges from the glass also contribute negative surface charges to some degree. Because the P(VDF-TrFE) films are very thin, photons could easily pass through, and so it may be that a large part of the contributed charge arises from the glass. On the negatively charged glass substrate, the P(VDF-TrFE) chains are immediately oriented perpendicular to the substrate when an electric field it applied—with the positively charged hydrogen atoms attached to the glass substrate, and the negatively charged

fluorine atoms repelled from the glass. As a result, stable spontaneous polarization arises within P(VDF-TrFE) films, which can be detected by the TSEE spectroscopy method.

IV. MOLECULAR MODELING, COMPUTATIONAL ANALYSIS, AND DISCUSSION

To explain these measured data and understand better the peculiarities of the PVDF and P(VDF-TrFE) copolymer molecular structures with regard to the different phase conformations, we performed molecular modeling and simulations using HypeChem 7.52 (Ref. 39) as well 8.0. We studied the dependences of the PVDF and P(VDF-TrFE) electrical properties (dipole momentum, polarization, energies of electron subsystem, as well as total energy of systems), both with and without applied electrical field, for molecular models of PVDF and P(VDF-TrFE) ferroelectrics with different lengths of the molecular chains and various conformations. The various computational methods were used, including first principles density functional theory (DFT) and semi-empirical calculations (such as PM3), as in restricted Hartree-Fock (RHF), as well in unrestricted Hartree-Fock (UHF) approximations. To obtain a better proof of results, we used various DFT methods, which are accessible in the HyperChem package, such as many-parameter exchange-correlation functional method HCTH98 (by Handy *et al.*[40]), Becke-88 functional[41] with Lee-Yang-Parr (LYP) correlation functional,[42] and Perdew-Wang-91 exchange functional[43] in combination with the fastest and most suitable PM3 semi-empirical method.[39] We used all of these for comparison of data. Both DFT approaches and the semi-empirical methods are widely used now, and have developed very rapidly,[44,45] but each have their own strengths and weaknesses. Because of this, it is an important practice to consider the most effective combinations of these different approaches.

We constructed and explored several minimal structural building blocks containing the two main (P = 2) PVDF copolymers $-CH_2-CF_2-$, or monomer units with TrFE variations, and for different conformation phases—trans (T) and gauche (G). We studied models with various lengths, and corresponding monomer number, P, variation, of the VDF copolymer units, including TrFE components (used to model P(VDF-TrFE) at a 70:30 ratio), and different conformations (T and G). We used, compared and analyzed both computational approaches. The details of these studies are prepared now for separate publication, but it was clearly shown that all computed data had a good agreement with those previously published,[16,17,31–37] which confirmed the validity of our computational approaches.

However, the main result, essential for the computational analysis of the TSEE experimental data in this paper, was the following: The computed energies of lower unoccupied molecular orbital (E LUMO) and electron affinities (EA, which corresponds to measured χ), especially their changes, are very close both for semi-empirical PM3 calculations and for DFT approaches (see Fig. 4). The energies of the highest occupied molecular orbital (E HOMO) and forbidden energy gap ($E_g = E\ LUMO - E\ HOMO$), computed by these two
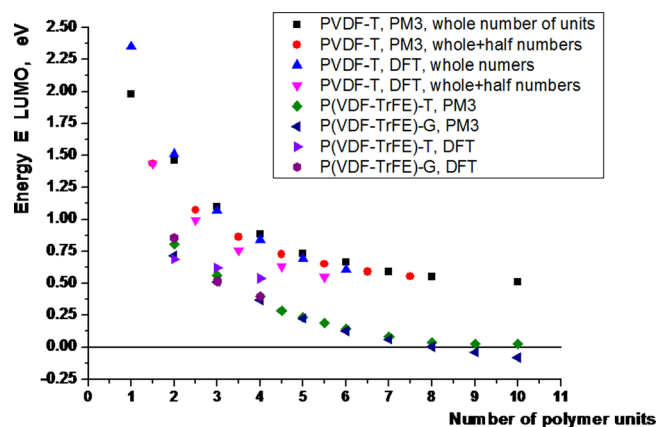

FIG. 4. Dependence of energies E LUMO vs. numbers of polymer units for different conformations (T and G), computed by various methods.

methods, are not in such good agreement, but their trends with increase in the number of monomer units in the PVDF and P(VDF-TrFE) polymer molecular chains are very similar, and have a good accordance with other published data. The results of DFT HCTH98 as well PM3 calculations are shown in Fig. 4 for E LUMO data, Fig. 5(a) for E_g, and Fig. 5(b) for E HOMO data. It can be seen that in an increase in the number of main polymer units leads to a decrease of energies for both E LUMO and E_g (Figs. 4 and 5(a)), corresponding to known data.[16,17] It is true for both methods used (PM3 and DFT), but while the E HOMO for PM3 is approximately twice the magnitude of that for DFT (Fig. 5(b)), the E LUMO energies are very similar for both methods (Fig. 4). From the data, we can conclude that for large chains (with numbers of units $\sim$5–10) there is little change in energy with increasing number, and for E LUMO there is little difference between the PM3 and DFT methods, although this is clearly not true for E_g or E HOMO (Figs. 4 and 5). In both E LUMO and E HOMO, the energy for various conformations is greater for T than for G, and is greater for PVDF than for P(VDF-TrFE). E LUMO reaches values of $\sim$0.5 eV for $\sim$10 chain units. Moreover, for large chains of P(VDF-TrFE)-T, the E LUMO values reach zero and even have a negative value for the G confirmation of the largest P(VDF-TrFE) chains (Fig. 4).

Based on these modeling data, by looking at E_g in Fig. 5(a), we can conclude that the greatest influence on the P(VDF-TrFE) chains of number >2 is due to the phase transition from T to G through additional thermo-excitation of the electron subsystem. This is connected directly with the E LUMO energies, corresponding to the bottom of the conductance band E_c and to the energy of EA (or χ in Fig. 1). Because the electron affinity and corresponding E LUMO energies are the most essential for the TSEE method used (i.e., the thermally excited electrons are emitted from the bottom of the conductive band or from the E LUMO level), we will focus on these points for the rest of this paper, using from now on the PM3 method, as was the fastest for these calculations.

For a deeper understanding of this process, we developed a model of the crystal cell, consisting of 10 monomer units in each polymer molecular chain, which corresponds to known data.[1–7,11,16,17] The resulting P(VDF-TrFE) double-cell
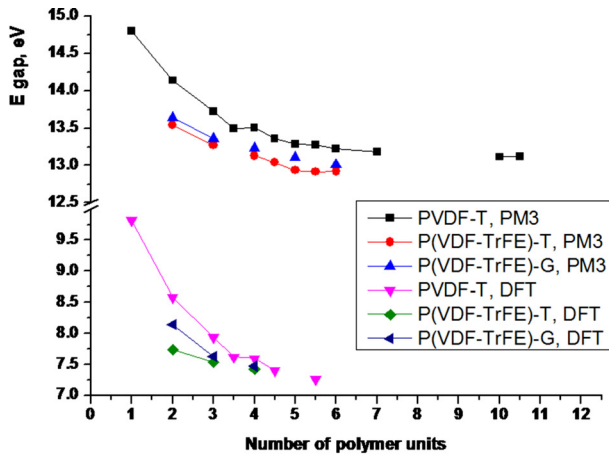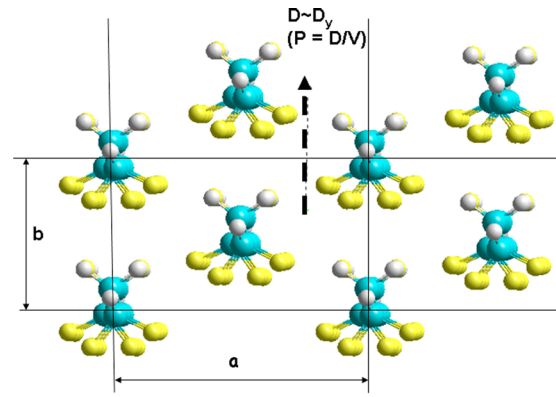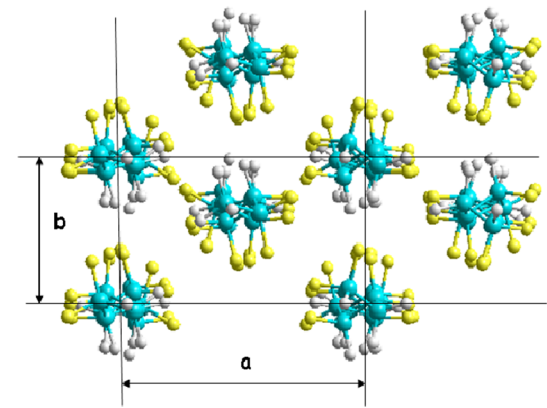
a)
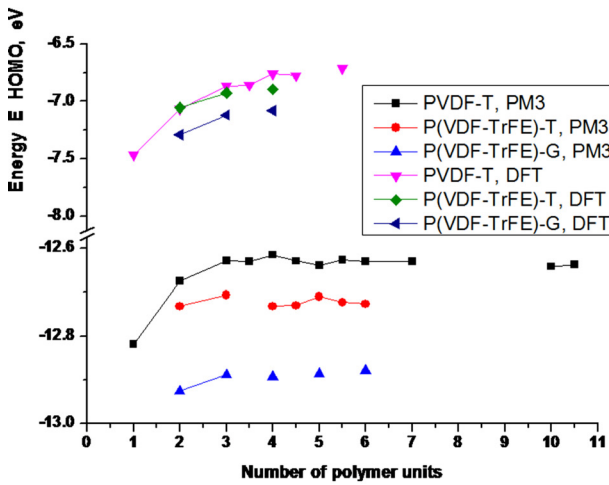
b)

FIG. 5. Energy dependence vs. numbers of polymers units: (a) energies of the forbidden zone E_g; (b) energies of the E HOMO.

a)

b)

FIG. 6. Model of the P(VDF-TrFE) cell in two conformations: (a) trans (T), (b) gauche (G).

structure models in both the trans (T) and gauche (G) conformations are shown in Fig. 6. We used the known cell parameters of $\mathbf{a} = 0.858$ nm, $\mathbf{b} = 0.491$ nm.[1–6,16,28,29] E LUMO, computed by the PM3 method, was ~ -1.568 eV (and E HOMO ~ -10.51 eV) for the stable T conformation of this model. The value of the total dipole moment, computed for this double-cell model in T phase, preferably oriented in the OY direction (corresponding to being perpendicular to the surface of a negatively charged glass substrate in the experimental conditions described above), is $D_t \sim D_y \sim 88.4$ D (in Debye units). The total volume of this double-cell molecular cluster, V_T, is ~ 1844.42 Å^3, and the value of the corresponding polarization, $P \sim P_y \sim 0.16$ C/m^2, compares well with known data.[1–7,16–18] The phase transformation to G phase, with a fully compensated dipole moment $D_t \sim D_y \sim 0$ D for the total double-cell volume $V_G \sim 1838.17$ Å^3, gives a zero value for the total polarization, $P \sim 0$ C/m^2. Values of the energies for G phase, computed by PM3, are the following: E LUMO ~ 0.0293 eV and E HOMO ~ -9.334 eV. Diagrams of these energy levels are presented in Fig. 7.

Therefore, from T to G we have a rise in E LUMO, with Δ(E LUMO) ~ 1.597 eV, and arrive at a near-zero final value of E LUMO, and a similar value for the electron affinity. If we compare these data with the TSEE experimental values above, we can see that the general order of values and the trends of their changes are verified (e.g., for the second sample we have a change of the work function from ~ 1.24 eV to ~ 0.08 eV, an affinity rise of ~ 1.16 eV). Because for TSEE the contributions of the thermalized electrons are the most essential, these electron energies play the key role in the TSEE processes.[26] Although the E HOMO computed by PM3 lies lower than that from DFT, the E_g obtained by PM3 is wider than that from DFT; nevertheless, the behavior and variation of the energies under phase transition from the T to G state of the modeled P(VDF-TrFE) have the correct features. That is, the energy of forbidden zone E_g is wider and all electron energies increase. The details of the changes of electron bands under an electric field for the transition between T and G states are shown in Fig. 7: E HOMO, E LUMO ($=$EA), Fermi energy E_F as half of forbidden zone E_g, as well the thermo-electron work function energy as sum of E_F and EA (or E LUMO).

The change of the total energy of the system for the molecular cluster in Fig. 6, consisting of 280 atoms (for the
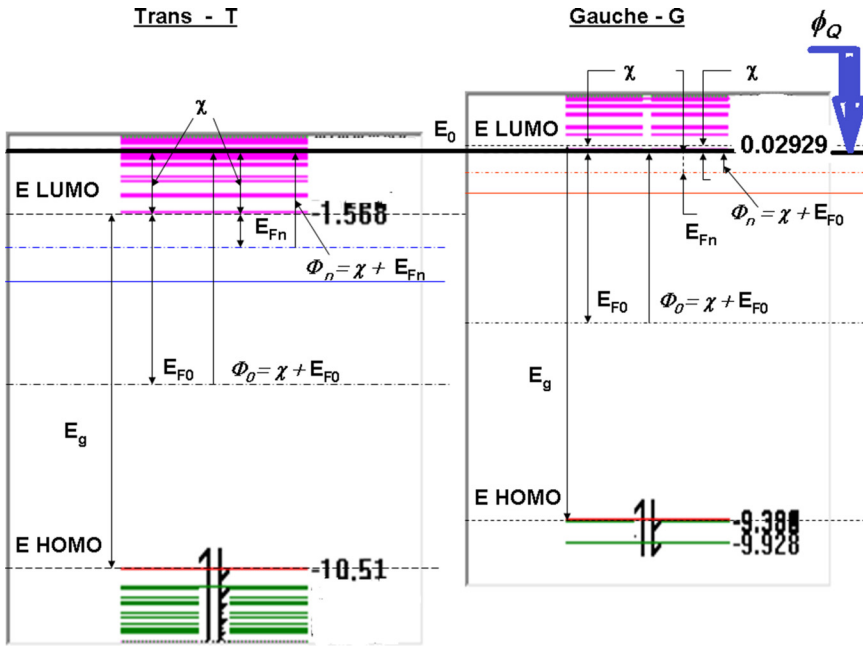
FIG. 7. Schematic of energies zones and their shift under influence of the electric field during phase transition between trans and gauche conformations. EA, electron affinity; E HOMO and E LUMO, highest occupied and lowest unoccupied molecular orbital, respectively; E_g, forbidden energy gap (E HOMO − E LUMO); $E_{f0} = E_g/2$; Φ, the energy level of the thermo emission electron work function ($\Phi \sim E_g/2 + EA \sim E_g/2 - E$ LUMO).

model of the P(VDF-TrFE) molecular cluster with 8 chains, $C_{11}F_{14}H_{10}$, with (VDF:TrFE) content of 70:30, and for T and G conformations), is $\Delta E_{T-G} \sim -1.97$ eV, ~ -46.5 kcal/mol, during phase transition. The equivalent total enthalpy change is ~ 58.18 J/g for the molar mass $M_c = 3265.424$ g/mol of these modelled systems.

The total energy is going down through transformation from T to G phase. However, because this transformation leads to a change in the configuration of each molecular chain and the total volume (volume in T state $V_T = 1844.42$ Å^3, while in G state volume $V_G = 1838.17$ Å^3), for a correct comparison we must look at the change in the energies density. This gives the following: $E_{vT} = -33.05034$ eV/(Å^3), $E_{vG} = -33.16379$ eV/(Å^3), $\Delta E_{v(T-G)} = -0.1135$ eV/(Å^3), or $\Delta E_{v(T-G)} \sim -2.62$ kcal/mol per volume. These changes correspond to the enthalpy of process $\Delta H \sim -3.35$ J/g (per volume unit, for the corresponding molar mass M_c, above). All these data compare well with many published values[37,46–50] and correspond to the T-G phase transition in the P(VDF-TrFE) (70:30) structure and crystal cell.

From other side, it is known that P(VDF-TrFE) has *n*-type semiconducting properties with corresponding energy of the Fermi level E_{Fn}, which is different from E_F in the middle of E_g, and is closest to the upper conductance band's lowest energy, E_c, or E LUMO[3,5,51,52]: $E_{Fn} \sim 0.8$–0.4 eV $<$ $E_F \sim 2$–4 eV (Fig. 7), shifted to the bottom of the conductance band (E_c and corresponding E LUMO energy). In this case, it is evident that after UV irradiation (with photon of energy $E_{pe} \sim 5.2$ eV–5.3 eV, close to the energy $E_g \sim 5.1$–5.6 eV[31–37]) these *n*-type levels would be excited and trapped as well. Consequently, the second irradiated P(VDF-TrFE) sample must manifest photo-ferroelectric[53] properties in this case.

This fact has real evidence here. If we analyze in more detail the TSEE spectrum data, compared with calculated energy levels (see Figs. 1, 2, 3, and 7), we can see that for the second sample, the thermo-emission electron work function energies Φ are shifted by the value of $\phi_Q \sim 0.64$ eV (in comparison to the first non-irradiated sample). Looking at the TSEE peak, after T_{max} the shift is $\sim 0.72 - 0.08 = 0.64$ eV, and before T_{max} the shift is $\sim 1.97 - 1.34 = 0.63$ eV. These are equal values if we ignore the 0.1 eV change on the glass surface, as mentioned above. This means that in these both cases (before T_{max} = in T state, and after T_{max} = in G state), for the second sample, an additional electric field exists inside the sample (from trapped charges in the surface levels) and has shifted all energy levels of system down in comparison to the "pure" ideal system without these additional levels (see Fig. 7). This field corresponds to the following estimated density of the surface charges: $N_Q \sim 7 \times 10^{12}$ 1/cm^2, which is very reasonable value[53] for common photo-ferroelectric materials. Therefore, our proposed model can also explain very well the photo-ferroelectric phenomenon, and this is an additional justification for the proof and validity of the computational approach developed for TSEE data analysis.

V. CONCLUSIONS

New developed computational molecular models of the PVDF and P(VDF-TrFE) ferroelectric polymers, especially the double-cell cluster model, are very useful for studies of the physical properties of this material at the nanoscale, and give us new data on the total energies, as well as for important electronic orbitals. The essential feature of the proposed model is that it can describe the phase transformation of these ferroelectric polymers from trans to gauche conformations and obtain the actual changes of the electronic energies and polarization. These data also compare well with experimental data. Most importantly, with this method and constructed model we can use a new application for the TSEE technique.

This new TSEE technique, in conjunction with these molecular modeling approaches, allows us to obtain the value of polarization, as well the data about electron affinity

and work function, of P(VDF-TrFE) samples undergoing the phase transition from T to G conformation when heated. The main advantage of this TSEE method is that it is a non-contact measurement, with no electrodes required, which can be very important and necessary for some applications. For example, in nondestructive *in situ* monitoring of a bone implant, especially with built-in sensors, it could give new information very necessary for control and further manipulations. Novel, smart nanobiotechnologies such as this could have wide ranging applications in contemporary and future nanobiomedicine.

ACKNOWLEDGMENTS

[1]L. Blinov, V. Fridkin, S. Palto, A. Bune, P. Dowben, and S. Ducharme, Phys. Usp. **43**(3), 243 (2000).

[2]A. V. Bune, V. M. Fridkin, S. Ducharme, L. M. Blinov, S. P. Palto, A. V. Sorokin, S. G. Yudin, and A. Zlatkin, Nature (London) **391**, 874 (1998).

[3]H. Qu, W. Yao, J. Zhang, S. Dusharme, P. A. Dowben, A. V. Sorokin, and V. M. Fridkin, Appl. Phys. Lett. **82**, 4322 (2003).

[4]H. Kliem and R. Tardos-Morgane, J. Phys. D: Appl. Phys. **38**, 1860 (2005).

[5]R. Tadros-Morgane and H. Kliem, J. Phys. D: Appl. Phys. **39**, 1 (2006).

[6]A. Gruverman and A. Kholkin, Rep. Prog. Phys. **69**, 2443 (2006).

[7]A. Tolstousov, R. Gaynutdinov, R. Tadros-Morgane, S. Judin, A. Tolstikhina, H. Kliem, S. Ducharme and V. Fridkin, Ferroelectrics **354**, 99 (2007).

[8]D. Li and D. A. Bonneli, in *Scanning Probe Microscopy: Electrical and Electromechanical Phenomena at the Nanoscale*, edited by S. V. Kalinin and A. Gruverman (Springer, New York, 2007), pp. 906–928.

[9]B. Rodriguez, S. Jesse, A. Baddorf, and S. Kalinin, Phys. Rev. Lett. **96**, 237602 (2006).

[10]B. J. Rodrieguz, S. Jesse, S. Kalinin, J. Kim, S. Ducharme, and V. M. Fridkin, Appl. Phys. Lett. **90**, 122904 (2007).

[11]V. S. Bystrov, I. K. Bdikin, D. A. Kiselev, S. G. Yudin, V. M. Fridkin, and A. L. Kholkin, J. Phys. D: Appl. Phys. **40**, 4571 (2007).

[12]S. J. Kang, I. Bae, Y. J. Shin, Y. J. Park, J. Huh, S.-M. Park, H.-C. Kim, and C. Park, Nano Lett. **11**, 138 (2011).

[13]S. Egusa, Z. Wang, N. Chocat, Z. M. Ruff, A. M. Stolyarov, D. Shemuly, F. Sorin, P. T. Rakich, J. D. Joannopoulos, and Y. Fink, Nature Mater., **9**, 643–648 (2010).

[14]Z. Hu, M. Tian, B. Nysten, and A. M. Jonas, Nature Mater. **8**, 62 (2009).

[15]S. Amer and W. Badawy, Curr. Pharm. Biotechnol. **6**, 57 (2005).

[16]V. S. Bystrov, N. K. Bystrova, E. V. Paramonova, G. Vizdrik, A. V. Sapronova, M. Kuehn, H. Kliem, and A. L. Kholkin, J. Phys.: Condens. Matter **19**, 456210 (2007).

[17]V. Bystrov, N. Bystrova, D. Kiselev, E. Paramonova, M. Kuehn, H. Kliem, and A. Kholkin, Integr. Ferroelectr. **99**, 31 (2008).

[18]A. Hereida, M. Machado, I. Bdikin, J. Gracio, S. Yudin, V. M. Fridkin, I. Delgadillo, and A. L. Kholkin, J. Phys. D: Appl. Phys. **43**(33), 335301 (2010).

[19]B. Callegari and W. D. Belangero, Acta Ortop. Bras. **12**(3), 160 (2004).

[20]R. Mehta, "The hip gets smart," Materials World Magazine, 1 April 2010, URL: http://www.iom3.org/news/hip-and-smart-biomaterials (data 17.07.2011).

[21]V. S. Bystrov, N. K. Bystrova, E. V. Paramonova, and Yu. D. Dekhtyar, Math. Biol. Bioinf. **4**(2), 7 (2009). URL: http://www.matbio.org/downloads_en/Bystrov_en2009(4_7).pdf.

[22]V. S. Bystrov, E. Paramonova, Yu. Dekhtyar *et al.*, J. Phys.: Condens. Matter. **23**, 065302 (2011).

[23]Yu. Dekhtyar, V. Bystrov, I. Khlusov, N. Polyaka, R. Sammons, and F. Tyulkin, in *The Society for Biomaterials 2011 Annual Meeting*, Orlando, FL, USA, 13–16 April 2011, p. A519 (2011).

[24]M. E. Lines and A. M. Glass, *Principles and Applications of Ferroelectrics and Related Materials* (Clarendon, Oxford, 1979).

[25]R. I. Minc, I. I. Milman, and V. I. Kryuk, Phys. Usp. (Russian) **119**(4), 749 (1976).

[26]Yu. D. Dekhtyar and Yu. A. Vinyarskaya, J. Appl. Phys. **75**(8), 4201 (1994).

[27]Yu. D. Dekhtyar, in *Functionalized Nanoscale Materials, Devices and Systems NATO Science for Peace and Security Series B: Physics and Biophysics*, edited by A. Vaseashta and I. N. Mihailescu (Springer Science + Business Media B.V., 2008), pp. 169–183.

[28]M. A. Marcus, Ferroelectrics **40**, 29 (1982).

[29]T. Furukawa, Ferroelectrics **57**, 63 (1984).

[30]K. Kimura and H. Ohigashi, Jpn. J. Appl. Phys. **25**, 383 (1986).

[31]R. E. Newnham, V. Sundar, R. Yumnirun, J. Su, and Q. M. Zhang, J. Phys. Chem. B **101**, 10141 (1997).

[32]J. Xiao, X. Zhou, Q. M. Zhang, and P. A. Dowben, J. Appl. Phys. **106**, 044105 (2009).

[33]J. Choi, P. A. Dowben, S. Pebley, A. V. Bune, and S. Ducharme, Phys. Rev. Lett. **80**(6), 1328 (1998).

[34]I. S. Elashmawi and N. A. Hakeem, Polym. Eng. Sci. **48**(5), 895 (2008).

[35]I. S. Elashmawi, E. M. Abdelrazek, H. M. Ragab, and N. A. Hakeem, Physica B **405**, 94 (2010).

[36]D. Mandal, K. Henkel, K. Muller, and D. Schmeiber, Bull. Mater. Sci. **33**(4), 457 (2010).

[37]E. Ortiz, A. Cuan, C. Badilo, C. M. Cortes-Romero, Q. Wang, and L. Norena, Int. J. Quantum Chem. **110**, 2411 (2010).

[38]V. I. Arbuzov, *Principles of Radiation Optical Materials Technology* (Saint Petersburg State University of Information Technologies, Mechanics and Optics, 2008) (in Russian).

[39]HyperChem.7.52, *Tools for Molecular Modeling* (Hypercube, Inc., 2002), URL: http://www.hyper.com/?tabid=360.

[40]F. A. Hamprecht, A. J. Cohen, D. J. Tozer, and N. C. Handy, J. Chem. Phys. **109**, 6264 (1998).

[41]A. D. Becke, Phys. Rev. A **38**, 3098 (1988).

[42]B. G. Johnson, P. M. Gill, and J. A. Pople, J. Chem. Phys. **98**, 5612 (1993).

[43]J. P. Perdew, J. A. Chevary, S. H. Volsko *et al.*, Phys. Rev. B **46**, 6671 (1992).

[44]Y. Zhao and D. G. Truhlar, Acc. Chem. Res. **41**(2), 157 (2007).

[45]J. J. P. Stewart, J. Mol. Model. **14**, 499 (2008).

[46]H. Su, A. Strachan, and W. A. Goddard III, Phys. Rev. B **70**, 064101 (2004).

[47]S. S. Guo, X. H. Sun, S. X. Wang *et al.*, Mater. Chem. Phys. **91**, 348 (2005).

[48]S. S. Guo, C. L. Sun, T. S. Wu *et al.*, J. Mater. Sci. **42**, 1184 (2007).

[49]W. Li, Q. Meng, Y. Zheng *et al.*, Appl. Phys. Lett. **96**, 192905 (2010).

[50]R. Gregorio, Jr. and M. M. Botta, J. Polym. Sci., Part B: Polym. Phys. **36**, 403 (1998).

[51]C.-G. Duan, W. N. Mei, J. R. Harfy, S. Ducharme, J. Choi, and P. A. Dowben, Europhys. Lett. **61**(1), 81 (2003).

[52]P. A. Dowben, J. Xiao, B. Xu, A. Sokolov, and B. Doudin, Appl. Surf. Sci. **254**(14), 4238 (2008).

[53]V. M. Fridkin, *Photoferroelectrics* (Springer-Verlag, New York, 1979).